Available online at www.sciencedirect.com

ScienceDirect

Ceramics International 35 (2009) 1747–1755

CERAMICS INTERNATIONAL

www.elsevier.com/locate/ceramint

Crack formation, exfoliation, and ridge formation in 500 °C annealed sol–gel silica coatings on stainless steel SUS304: Part II Spectroscopic and mechanical analyses and insights into mechanisms controlling coating characteristics

Makoto Takemori *

Research Institute for Environmental Management Technology, National Institute of Advanced Industrial Science and Technology (AIST), 16-1, Onogawa, Tsukuba 305-8569 Japan

Received 5 May 2008; received in revised form 3 July 2008; accepted 30 September 2008
Available online 5 November 2008

Abstract

This report is a continuation of Part I of my studies of a non-aqueous sol–gel silica coating deposited on stainless steel SUS304. Part I discussed the microscopic observation of cracks, ridges and interlayers within the resulting silica coatings, and provided limited insight into their respective mechanisms of formation. This report provides further explanation for the mechanisms of these processes, as evidenced by spectroscopic and nano-indentation analyses of the coatings. Specifically, the coatings were analyzed by Fourier transform infrared spectroscopy, X-ray photoelectron spectroscopy, X-ray diffraction, and Auger electron spectroscopy. These results are discussed along with those obtained in Part I to further assess the mechanisms of crack formation in the coatings, and it was found that coating shrinkage and tension most likely caused crack formation. It seems that the O-deficient interlayers were formed under a mild oxidation condition existed around the silica/SUS304 interface during ~500 °C annealing. Additionally, nano-indentation analysis indicated that the coatings were compact, but the coatings' hardness was intermediate. Suggestions for improvement of sol–gel silica coatings on stainless steel are also provided.

Keywords: A. Films; A. Sol–gel processes; B. Interfaces; D. SiO_2

---

1. Introduction

In the previous report (Part I), substantially thick (~1 μm) non-aqueous sol–gel silica coatings deposited on SUS304, which should be useful in many applications, were observed by microscopy to be of 'good-quality,' that is, compact, uniform, adherent, sufficiently hard, smooth, without excessive organic or moisture content, and transparent. In Part I, mainly structural and compositional results and their interpretations were described. Notably, the thicknesses of the silica films ranged from ~350 to ~1000 nm. The films were largely uniform, compact, and adherent, with few organics remaining in the films after the 500 °C annealing process. However, the films contained both shallow and deep cracks as well as exfoliated sites. In some cases the cracks were rather shallow, terminating without approaching the SUS304 substrate. The lateral propagations of the deep cracks were basically independent of the occurrence of ridges or pre-existing scratches in the SUS304 substrate. Nevertheless, some shallow cracks were observed to follow ridges that had evolved in the silica coating.

In addition, three consecutive interlayers were formed during the annealing process. The innermost one was ~5 nm thick, Cr-rich, highly O-deficient, and formed a tenacious bond between SUS304 and silica; the two others were rather diffuse and less O-deficient. Many ridges formed in the silica coating near its interface with the SUS304 substrate. Most of the ridges were accompanied with SUS grain boundaries. Ni was almost absent in silica coating except in the innermost interlayer and ridges.

The aim of this part of the report is to further consider these aforementioned findings in the context of mechanical testing and spectroscopic characterizations. In particular, nano-

---

* Tel.: +81 29 861 8180; fax: +81 29 861 8459.
E-mail address: takemori.mkt@aist.go.jp.

0272-8842/$34.00 © 2008 Elsevier Ltd and Techna Group S.r.l. All rights reserved.
doi:10.1016/j.ceramint.2008.09.015

indentation analysis was performed on the coated SUS304 substrates, and the results are discussed here. Additionally, a host of spectroscopic analyses were performed on the samples, including Fourier transform infrared spectroscopy (FT-IR), X-ray photoelectron spectroscopy (XPS), X-ray diffraction (XRD), and Auger electron spectroscopy (AES). The results of these studies, along with those of the microscopic observations presented in Part I, are discussed here in terms of crack initiation, propagation, and termination mechanisms. Additionally, the formation and properties of the three consecutive interlayers are also discussed. On the basis of these experimental results and discussions, suggestions for the improvement of sol–gel silica coating on steels, especially Cr- and Ni-containing steels, such as SUS304, are proposed.

2. Experimental procedures

2.1. Sol–gel coating

The samples used here for mechanical testing were prepared from the same materials and by the same means as those used for Samples 1 and 2 in Part I of this report. Substrates were coated with silica according to the non-aqueous sol–gel method reported previously [1]. Briefly, 20-ml portions of tetraethylorthosilicate (TEOS) and acetic acid were mixed and then heated at ~120 °C for ~60 min; then, 20 ml n-hexane was added and the mixture was again heated at ~120 °C for ~60 min; finally, a second 20-ml portion of n-hexane was added and the mixture was heated at ~120 °C for ~450 min. The SUS304 plates were dipped in the resulting solution, and the dip-coated substrates were heated in air atmosphere from room temperature to 150 °C (temperature not programmed exactly but reached in ~26 min and kept for ~94 min). The temperature then was raised to 190 °C (reached in ~15 min and kept for ~825 min) before the plates were cooled in the furnace, soaked in water for about 5 h, heated again at 190 °C (reached in ~37 min and kept for ~803 min), and cooled again in the furnace. This process is referred to herein as the 'first heating process'. The samples were then heated in air from room temperature to 500 °C at 5.5 °C min^{-1}, kept at 500 °C for 120 min, and then cooled in the furnace. This process is referred to herein as the second heating process.

For Samples 1 and 2, SUS plates of 50 mm × 50 mm × 1 mm-thick dimensions were used immediately after removal of their protective polymer films and washing with ethanol. The samples were vertically suspended during the dip-coating and the first heating process, and then placed horizontally in the furnace for the second heating process. (The withdrawal rate of dip-coating was ~10 mm/s. The dip-coated parts were ~15 mm from the lower edge, and the upper parts remained uncoated, but these parts were treated without separation afterward in the coating treatments.)

2.2. Characterization

Samples 1 and 2 were previously characterized by various microscopy techniques, as described in detail in Part I of this report.

For this section of the report, Sample 1 was mechanically tested by means of nano-indentation. A nano-indentation apparatus (Nano Indenter XP; MTS Ltd.) with data-analyzing software (Test Works 4) was used for nano-indentation analysis of Sample 1, which was not cut prior to analysis. For each set of nano-indentation analyses, 15 points were measured and not more than 4 bad data points were neglected.

Sample 2 was characterized by means of Fourier transform infrared spectroscopy (FT-IR), X-ray photoelectron spectroscopy (XPS), X-ray diffraction (XRD), and Auger electron spectroscopy (AES). The sample was mechanically cut into appropriately sized pieces with a dicing saw using water before analyses. For FT-IR analyses, two 100 μm × 100 μm areas of each location were analyzed by attenuation total reflection (ATR) with a spectrometer (Paragon 1000-Auto-IMAGE System; PerkinElmer Inc.). The selection of the FT-IR analysis areas is described in Section 3.2. For XPS analysis, a spectrometer (ESCA-K1; Shimadzu Corp.) with Mg Kα irradiation and Ar^+ sputter-etching was used. An X-ray diffractometer (RINT 1500; Rigaku Corp.) with Cu Kα X-rays was used for XRD measurements. The incidence angle was fixed at 1° from parallel to the surface to acquire data sensitive to the coating film as compared to the substrate.

For AES, both exfoliated and unexfoliated portions of the sample surface were analyzed with a spectrometer (PHI 670; PHI Inc.). The area of each AES analysis was ~30 μm × 30 μm, and AES spectra were acquired before and after a slight sputter-etching by Ar^+.

3. Results

3.1. Nano-indentation results

Nano-indentation analyses were performed for three morphological regions of Sample 1: a region near a deep crack, one near an exfoliation site, and one near neither a deep crack nor an exfoliation site. Fig. 1(i) and (ii) shows the depth dependence (strictly speaking, the diamond head displacement dependence) of the Vickers hardness, Hv, and Young's modulus, E, respectively. The results were characteristic of a compact silica film rather than of a sol–gel derived porous silica film [2], and the profiles for the three regions were basically similar to one another. Both representative Hv values at a depth of 100 nm and representative E values at the profile's shoulder were almost the same for the three regions, but both of these sets of values were only ~25% as large as the values reported for thermally grown silica (Hv = 8.5 GPa, E = 70 GPa) [2]. At larger depths (>~200 nm), both Hv and E were a little smaller (i.e. softer) for the region of the coating near an exfoliation site than for other two regions.

3.2. FT-IR results

Fig. 2 shows FT-IR data obtained from a region of Sample 2 not near any apparent cracks. A nearly identical spectrum was

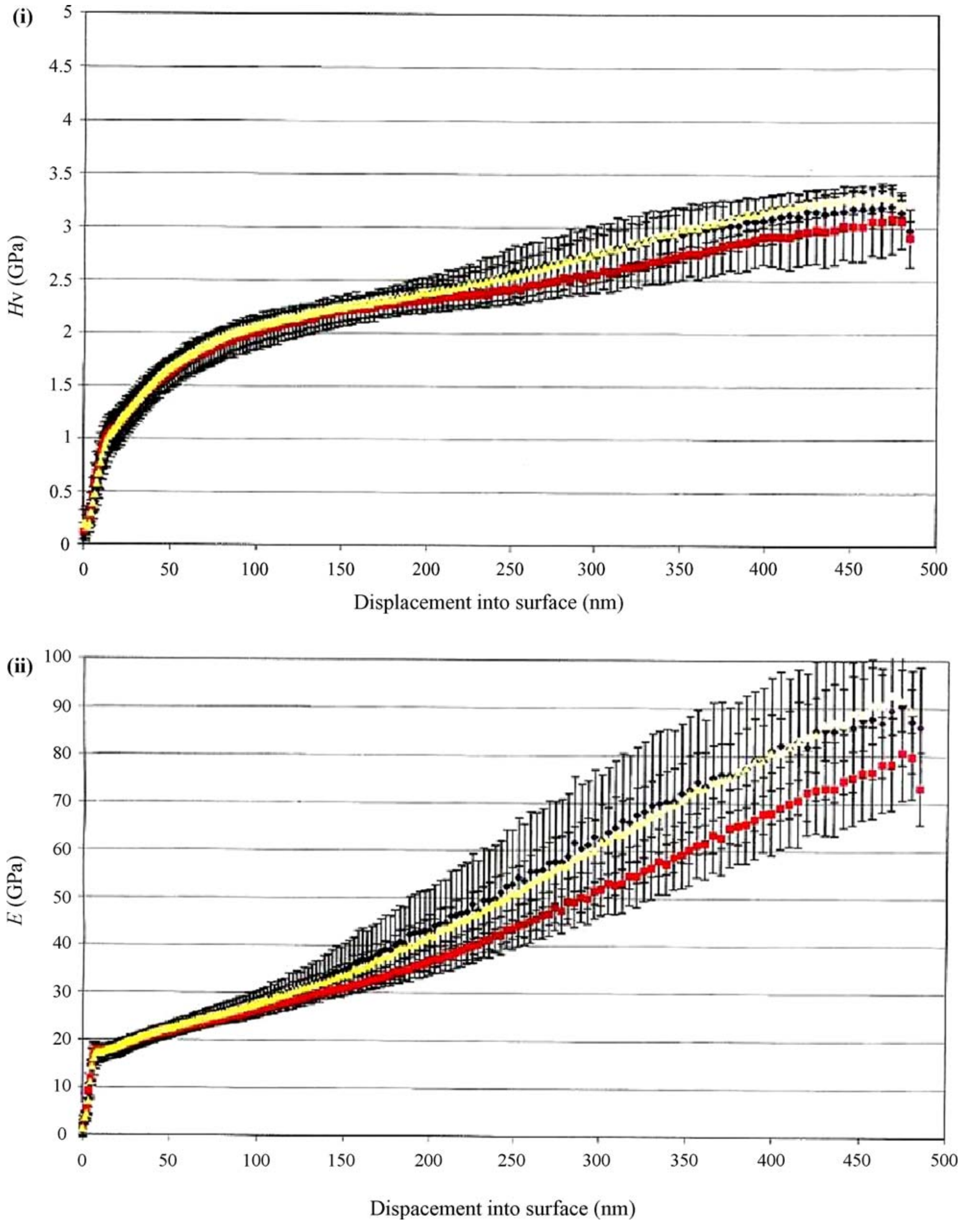

Fig. 1. Nano-indentation results for Sample 1. Dependence of (i) Vickers hardness and (ii) Young's modulus, as functions of diamond head displacement into three regions of the sample, with error bars (black: region near a crack; red: region near an exfoliation site; yellow: region near neither a crack nor an exfoliation site) (For interpretation of the references to colour in this figure legend, the reader is referred to the web version of the article.).

obtained from a region near a crack. The peaks around 1000–1250 cm^{-1} (ascribed to Si–O–Si bonding) were clearly resolved. The sharpness of the most prominent peak at 1036 cm^{-1} was also characteristic of the present silica coating.

3.3. XPS results

The XPS results in Fig. 3 show a red-shift of the Si 2p peak from 103.5 to about 99 eV, concurrent with Ar^+ sputter-etching approaching to and going beyond the thin interlayers. Carbon (probably a contaminant) was present on the topmost surface but soon disappeared with sputter-etching.

3.4. XRD results

XRD results for Sample 2 (data not shown) showed a broad peak centered at 22°, which is characteristic of amorphous silica, and a small peak near 45° ascribed to SUS304.

3.5. AES results

For both exfoliated and unexfoliated regions of Sample 2, a substantial amount of C (probably as a contaminant) was present. Apart from C, only Si and O were detected at the surface of the unexfoliated coating, but a large amount of Fe,

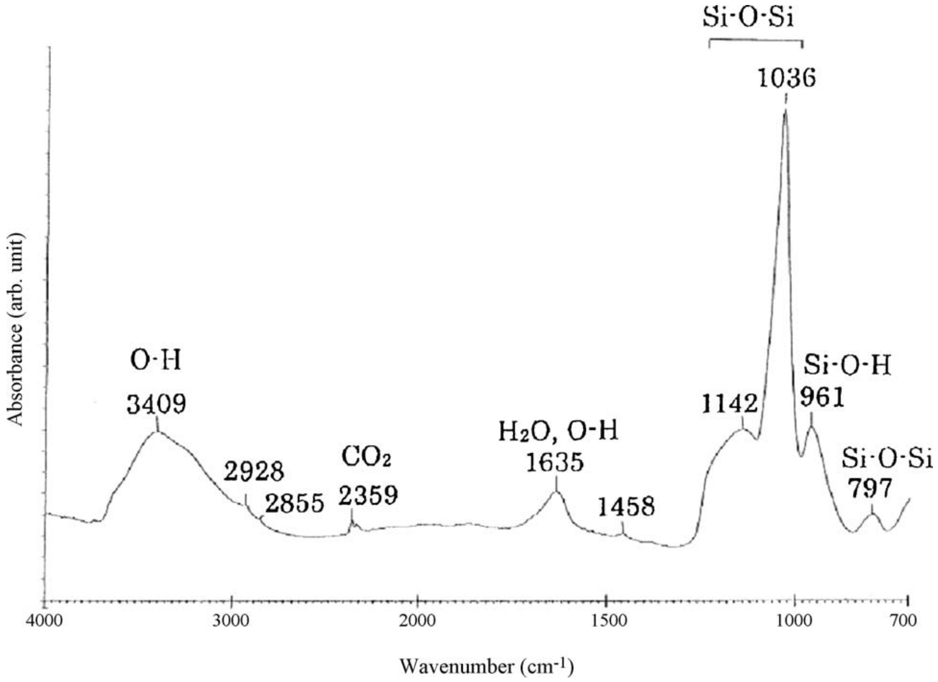

Fig. 2. FT-IR spectrum of a region of the Sample 2 silica coating not located near a crack.

and O and a small amount of Si were observed at the exfoliated surface. After the slight sputter-etching, AES spectra from both regions were basically unchanged except that C peaks were reduced.

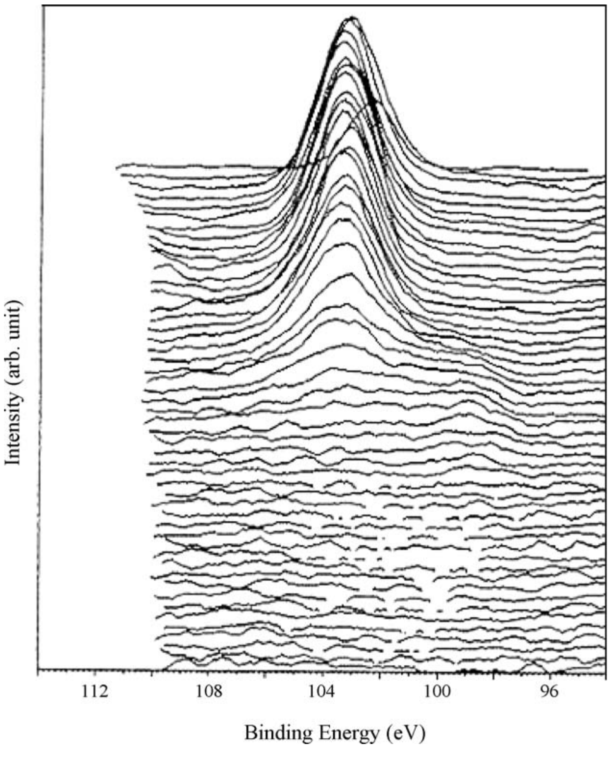

Fig. 3. XPS spectra of Si 2p during Ar^+ sputtering of Sample 2 (from top to bottom in sequence).

4. Discussion

4.1. Interpretation of nano-indentation results

Nano-indentation results indicated that the cracks did not appear to have preferentially initiated in macroscopically softer or harder regions of the samples. Nano-indentation results showed that the mechanical properties were almost indistinguishable between sample regions located far from deep cracks and sample regions located near a crack. However, the film was a little softer at large-depth nano-indentation analyses performed near exfoliation sites, suggesting that the ‘softness’ in these deeper regions likely resulted from exfoliation, rather than caused crack initiation.

4.2. Interpretation of FT-IR results

The FT-IR spectra mostly represented the nature of the silica matrix and not that of sub-oxides, because sub-oxides were present only as thin layers near the SUS304 substrate, as shown by the XPS results, as well as the TEM/EDX results presented in Part I. Additionally, information about the sub-oxides must have been greatly attenuated, because the thickness of the coating (~1 μm) was comparable to or greater than the probe depth of ~500 nm usually afforded by ATR-IR [3,4].

The clear splitting of the two peaks around 1000–1250 cm^{-1} (ascribed to Si–O–Si bonding) and the sharpness of the prominent peak at 1036 cm^{-1} are characteristic of the present samples. The observed peak splitting likely indicates macroscopic tension, because such splitting is typically correspond when preparative conditions that promote tension are used, such as shrinkage of coatings during heating [5], or centrifugal spin coating introducing shear stress and subsequently accompanying tension [6]. Furthermore, samples that are not subjected to tension-inducing conditions, such as samples prepared in the absence of macroscopic stress [7] or swelling of coating by oxidation [8], typically do not exhibit peak splitting. Peak splitting in this wavenumber region has also been reported for thin (<80 nm) silica films formed on Si by oxidation [9], but such films cannot be directly compared to the present samples because in such thin films, large compressive stress caused by increasing volume cannot be avoided and oxygen deficiency is scarce [10].

Peaks ascribable to C–H around 1380 and 2850–2950 cm^{-1} were not prominent, but peaks assigned to O–H, H_2O, and CO_2 were clearly present. I believe that the majority of these species as detected ex situ by XPS as well as FT-IR must have been contaminants, both because C was detected only on the topmost surface by XPS, and because clear occurrence of irregularities (e.g. voids and cracks of large or small size) in the silica matrix indicative of significantly incorporated humidity [11] did not take place at least in the later stages of the 500 °C annealing process. However, a large amount of moisture might have been incorporated into the silica coating after cooling under conditions of tension [12].

4.3. *Presence and effects of stress*

The features of the films observed by OM and SEM and the preparation conditions (in which film shrinkage was expected via escape of humidity and organics) strongly suggest that tension was induced during the ~500 °C annealing process (see Part 1). The FT-IR spectra also indicated the presence of tension, although this data was ex situ. But the sign of the stress (i.e. tension or compression) in the sample probably did not vary in the time between the annealing process and the collection of the FT-IR data, because the thermal expansion coefficients of sol–gel driven silica that has been heated above ~400 °C are generally small [13], smaller than those of SUS304, meaning that tension in the film could not have increased during cooling. Additionally, the incorporation of humidity into the silica film after annealing [12] would not have increased the tension. Then it follows that tension must have been more intense in situ than ex situ. By the way, it has been reported that addition of small amounts of water vapor into the environment during silica coating at high temperatures can relax stress in coatings [14]. In the present study, however, although water vapor was not removed from the environment air during the ~500 °C annealing, tension was still operating (i.e. not thoroughly relaxed).

The effects of stress, other than those relating to the initiation/propagation of macroscopic cracks, are rather ambiguous, but plausible effects of expected compression around the innermost and the second innermost interlayer are described in Part 1, Sections 4.1.2 and 4.2 of this report (i.e. termination/diversion of vertical cracks and healing of nanoscale defects in these interlayers, respectively). I also suspect that the lateral tension in the coating might have introduced microscopic layer-like structures oriented nearly parallel to the SUS304 substrate by arranging rigid ring structures borne in the silica matrix during high temperature annealing; these structures could have blocked diffusion of O across the silica film and contributed to the establishment of an O-deficient region near the SUS304 substrate, as described also in Section 4.1.2 of Part I (and also just below in Section 4.4 of Part II). Such layer-like structures are not clearly evident in the present samples, but the formation of a birefringent sol–gel silica film by spin coating has been reported [6], suggesting that layer-like structures are formed on some sol–gel silica films under conditions with tension. Interesting simulations of small and rigid silica rings orientated parallel to the stress axis (although uniaxial) [15] also have been reported. Moreover, precipitation of sheet-like silicates from liquids composed of TEOS and surfactants [16], and O-barrier effects of silica coatings prepared from liquids by layer-by-layer deposition methods (although without artificially applied stress) [17] have been reported. If these assumptions of 'tension induced layer-like microscopic structures' are valid, then the silica matrix observed here also could have been mechanically strengthened to some extent, because it is well known that layer-like structures are usually tough toward fracturing across the layer [18].

The stress within the present silica films could have also affected the bulk diffusion of elements and species other than internal OH groups and O [19], but this effect is ambiguous in the present case. Stress-induced surface corrugation has been reported for systems in which surface diffusion is dominant [20], though such corrugation was not clearly observed here.

Raman spectroscopy in situ could provide more direct information about stress and atomic-scale structures in these silica films [21]. This characterization should be performed in future experiments.

4.4. *Formation and properties of the three consecutive interlayers*

The formation of interlayer(s) between silica coatings and stainless steel substrates has been suggested previously [5,22]. In the present samples, three consecutive interlayers were observed. Because samples after the first heating process had a luster not quite different from that of untreated SUS304, these interlayers must have formed mostly in the second (~500 °C) heating process. I propose that the interlayer formation occurred by the following six-stage process, although the stages could have been overlapped to some extent.

4.4.1. *1st stage*

A small amount of metallic elements in SUS304 was moderately oxidized at the silica/SUS304 interface.

4.4.2. *2nd stage*

The mixed metal ions split into two groups: one group was Fe-rich, and the other was Cr-rich. Each group formed a rather diffuse interlayer and slowly migrated outward, with the migration speed for the Fe-rich interlayer being faster than that for the Cr-rich one.

4.4.3. 3rd stage

The third and innermost interlayer, which was highly O-deficient, gradually formed adjacent to SUS and did not migrate.

4.4.4. 4th stage

After the innermost interlayer grew to about a 5-nm thickness, further oxidation of metallic elements in SUS304 almost stopped, with the exception of elements located near the nano-sized defects formed by some causes. The two diffuse interlayers then continued to migrate outward without any additional supplementation of metal ions from SUS304.

4.4.5. 5th stage

The distances between the three interlayers gradually increased.

4.4.6. 6th stage

The diffusivity decrease of O,O-related species and metallic elements in the silica matrix eventually caused the evolution of all three interlayers to stop (see Part I).

The innermost layer not only promoted adherence of the silica film (as described in Part I) but also must have hindered oxidation of the SUS304 substrate. Reportedly, SiO_x is expected to act as a diffusion barrier for O [23], for Ni [24], and in some conditions for Fe [25]. Contrary to the report by Vasconcelos et al. [5], the penetration of O into the SUS304 substrate was not abundant in this case. This observed lack of O-penetration can be explained in terms of the compactness and diffusion barrier effect of both the innermost interlayer and the silica matrix itself. Also, in spite of the reported hardness (or brittleness) of O-deficient SiO_x [26] and CrO_x [27], the innermost interlayer seems to have remained compact and uniform under the conditions of the present study, where moderate strength of compression is strongly suggested (see Part I, especially Sections 4.1.2 and 4.2).

Nevertheless, some uncertainties remain with this study. For example, the possibility that the innermost interlayer condensed from a rather diffuse layer (e.g. by means of reduction by non-oxidized Cr or Si in SUS304) cannot be eliminated completely. Additionally, whether the Si in the interlayers came from SUS304 or from the silica matrix is ambiguous. However, the decrease in Si content in the region of SUS304 adjacent to the innermost interlayer, shown in Part I, Table 2, strongly indicates that at least some part of Si in the innermost interlayer came from SUS304.

Questions also remain concerning the roles of various metallic elements in the formation of a good-quality silica coating. In particular, the roles of Fe are rather complicated, but probably not detrimental to the stability and adherence of the innermost interlayer rich in both Cr and Fe. Such effects are suggested because steels containing a moderate amount of Cr reportedly have better oxidation resistance than those containing higher amounts of Cr [28]. Additionally, the reason for the observed high Ni content only in the innermost layer, as well as Ni's possible activity in the innermost layer, is also unknown. I speculate that highly O-deficient Cr–Fe–Si–Ni sub-oxides exhibit unique mechanical and chemical properties, e.g. adherence to SUS and silica, and diffusion barrier effects for O and metallic elements. Phenomena of diffusion of elements, such as O [29], Fe [30], Cr [31], and Ni [32], as well as of electron migration [31], in amorphous silica, silica gel, and SiO_x are complicated. Intensities of diffusing elements as well as diffusion mechanisms might have changed during the course of annealing, owing to the vast changes in the silica (gel) structure. Oxidation mechanisms of metallic elements and organics, escaping routes of oxidized organics and humidity, and the porosity of the silica matrix (if any) might also have changed during annealing. Other characterization methods, such as positron annihilation [33], are required to clarify whether very small (<2 nm) micro-pores existed in silica, and whether such micro-pores were isolated or interconnected.

Questions concerning the roles of C and H also cannot be neglected. As described in Part I, the innermost and the next innermost interlayers are degraded near substrate SUS304 grain boundaries where C and H both are expected to play important roles [34–36]. Hydrogen has been shown to be important also in relation to sub-oxides [37].

It is interesting and practically important to clarify under what conditions interlayers like in the present study are formed between silica coating and substrate SUS of various types. Hänni et al. [38] reported that for thick silica coatings prepared by thermal decomposition of TEOS on AISI316L, two interlayers were observed: the inner one consisted of $(Fe_{0.45}, Cr_{0.55})_2O_3$ and the outer one consisted of Fe_2O_3. These species are not likely to be O-deficient. In their report, voids were found between the two interlayers and guided cracks to propagate. That is to say, there is not a single mode for formation mechanisms and natures of interlayers between silica coating and SUS substrate. Further studies should investigate whether these different modes shift from one to another gradually or abruptly with changes in conditions of preparation or usage.

Furthermore, the stability of the silica coatings in the present study has not been fully elucidated. Although decomposition of SiO_x by Fe has been reported [39], no distinct degradation of sub-oxides was observed in the present study. And the local degradation of the interlayers was automatically cured to some extent, i.e. at ridge parts nanoscale defects introduced into sub-oxide interlayers later being cured by themselves, as described in Part I.

4.5. Suggestions to improve silica coating on Cr-containing steels

On the basis of the results both here and in Part I of this report, I now propose the following keys for producing better quality silica coatings of several μm thick or more on Cr-containing steels, such as SUS304. First, tenacious Cr-rich sub-oxide interlayer(s) that are free of both nanoscale and larger defects are crucial for the formation of effective silica coatings. These interlayers should be not thick, but compact; they should be adherent; serve as good barriers for diffusion of O, Fe, Cr, and Ni; and curable by itself when nanoscale defects were introduced; and stable during treatment and in practical application. To meet these requirements, modestly intense oxidizing conditions of SUS in contact with silica-based coatings should be controlled by means of programmed heating or other methods, such as control of the gas environment during annealing. Additionally, SUS substrates used for such preparations should contain a minimal mechanical scratches. SUS with low C content may be preferable because C in SUS is the most highly suspected element in SUS to cause ridge formation, as described in Section 4.2.2 in Part I. SUS moderately enriched (or implanted) with Si [40], N, and rare earth metals [40] may be worth exploring for use as a substrate, because these types of SUS often show excellent oxidation resistance, which is one of the most important requirements for good quality silica coating on SUS.

To further improve the quality of silica coatings on SUS substrates, coating liquids should be developed that produce films that are less prone to the formation of cracks and pores and to exfoliation during annealing. These liquids should be homogeneous, but with a silica concentration as high as possible. The wettability between the liquid and the substrate is also important, and the gelling time (or 'pot life') of these silica solutions should be sufficiently long. The addition and internal synthesis of small amounts of organic species, such as polyvinylbutyral [41] or surfactants [1], to the silica solutions is a synthetic strategy worth testing for improvements especially in adherence and uniformity of the coating. During annealing, not only good adherence should be maintained, but the rigidity of the silica matrix should increase without becoming brittle, and the diffusivity of O should decrease.

In addition to the suggestions proposed above, the incorporation and nucleation of distinct particles in the coating should be prevented. Processing in a clean box or a clean room is desirable for the prevention of such particle incorporation. In the present study, the first two proposed suggestions were largely adhered to, which might explain the observed good quality (although not sufficient) of the silica coatings. By preparing these films by means of the sol–gel method in a cleaner environment, perhaps better quality films could be attained.

If the treatment conditions described in Section 1 were permitted to be loosened, many other reported strategies for the improvement of silica coatings could be explored. For example, (pre)treatments using Si–C-containing species [42], silazane [43], solutions containing rare earth metals [44], SiO_x [45], or N-containing organics other than silazane [46] might be effective. Although excessive Si–C bonding can increase the presence of undesirable properties, such as O permeation [47] and film softness [48], it has been previously demonstrated that the addition of a small amount of simple polydimethylsiloxane to a coating solution can effectively increase the 'pot life' of the solution to a period exceeding several months [49]; the liquid is wettable to a variety of substrates and its silica content was more than that of pure TEOS. (I am currently investigating methods using this type solution to further increase silica content without shortening the 'pot life'.) By the way, as with methods using silazane interestingly, Pêcheur et al. [50] reported that the stresses in silica coatings prepared by plasma-enhanced decomposition of hexamethyldisilazane easily relax at temperatures as low as 100 °C. Silica films with 'good quality' (~1 μm thick, Hv = 3.2 GPa, $E = 33$ GPa) prepared from silazane at room temperature are available [51].

Okuzaki et al. reported rigidity increase of sol–gel silica coatings after ultraviolet light irradiation [52]. The treatment of silica liquids and coatings with ultrasound [53], magnetic fields [54], or both is worth testing for improvement of adherence. The combination of glass lining technology [55] with non-aqueous sol–gel methods may also be possible. Surface pretreatment of SUS using ozone or laser (or both) is interesting, because the former is reported to bare tenacious Cr-rich amorphous oxide scale films as low as 200 °C [56], and the latter to bare corrosion resistant surfaces even when carbonized SUS was chosen [57].

Still other alternative methods are possible. Removal of abundantly coexisting (semi)metallic elements other than Si (e.g. B [58], Al [59]) in the course of the sol–gel thick silicate coatings on steels by some chemical methods can be one of them, as far as remaining a small amount of these extra (semi)metallic elements are tolerated in particular applications. Addition of external fiber-or sheet-like powders of nanoscale in width or thickness into the sol–gel coating solution may be another possible method in applications where uniformity is not strictly required. Developments of electrophoretic sol–gel coating methods with eliminated problems related to electrodes may be also important.

Summarizing from another viewpoint, there are two major requirements to obtain appreciably thick (much more than 1 μm) and 'good quality' silica coatings on substrates, such as SUS304. One is the preparation of high-silica-containing sol–gel liquids of good homogeneity and adherence to the substrate steels, and this is already accomplished to some extent by non-aqueous sol–gel methods. The second requirement is more complicated, that is, achieving compatibility between the following four conditions during annealing: relaxed tensile stress in the silica matrix; retained diffusion barrier effects; fairly high rigidity evolving in the silica matrix; and retention of adherence. To solve this problem, strategies, such as those described above and their hybrids are possible; by doing so, crack formation and eventual exfoliation may be eliminated.

Within the loosened preparation conditions probably, irrespective of some difficulties arising from silazane, hybridization of silica-enriched non-aqueous sol–gel methods with a little amount of silazane treatments (e.g. pre- and/or post-treatment with silazane, and/or addition of silazane into the coating liquid) may be one of the most possible and practical methods.

5. Conclusions

Silica films were formed on SUS304 by means of a previously studied non-aqueous sol–gel method. The coated specimens were annealed at 500 °C and analyzed by a variety of microscopic, spectroscopic and mechanical techniques, yielding the following conclusions:

(1) FT-IR results confirmed that tension was operating in the silica coating, but most probably not near the interface with SUS. The tension was apparently stronger in situ than ex situ. This observation was confirmed by microscopy in Part I.
(2) Nano-indentation analyses indicated compactness of the unexfoliated silica coating, but both the Vickers hardness and Young's modulus were about 1/4 the values observed for thermally grown, compact silica films. The hardness of the silica coating was a little less at near the exfoliation than far from exfoliation.
(3) XPS results confirmed that Si at the innermost interlayer was in the sub-oxide state, as suggested by TEM/EDX data in Part I.
(4) XRD results indicated that the silica coating was mostly amorphous.
(5) AES results confirmed that Fe, Ni and Cr were not present near the outer surface of silica coating.
(6) As shown in Part I, three consecutive interlayers existed between silica coating and SUS. It seems that they were formed by a six-stage process including chemical reaction between silica coating (liquid/solid) and SUS304, diffusion of metallic/non-metallic elements/species and evolution of micro-/mesoscopic structure in the interlayers and silica matrix. The innermost layer not only promoted adherence of the silica coating (as described in Part I) but also must have hindered oxidation of the SUS304 substrate. It is speculated that the innermost interlayer consist of highly O-deficient Cr–Fe–Si–Ni sub-oxides exhibited unique properties. Local degradation of the interlayers seems to have been automatically cured to some extent.

On the basis of these conclusions, some suggestions have been proposed to improve the quality of silica coatings on SUS. These suggestions include the surveying of more appropriate treatment conditions and selection of SUS for tenacious interlayer formation; the further development of high-silica-content, adhesive, and homogeneous coating solutions; and the prevention of dust particle incorporation into the coating liquid before/during preparation.

Acknowledgements

I gratefully acknowledge the useful discussions with and cooperation of researchers and staff of the AIST (National Institute of Advanced Industrial Science and Technology), Kobe Steel, Kobelco Kaken Co., Ltd., NSG Techno-Research Co., Ltd.

References

[1] M. Takemori, Low temperature synthesis of a silica-based glass-like adherent film by a sol–gel method, J. Mater. Sci. Lett. 20 (2001) 151–154.
[2] A. Nakaue, N. Kawakami, Evaluation of the mechanical properties of thin films using nanoindentation, R-D Kobe Steel Eng. Rep. 52 (2) (2002) 74–77 (in Japanese).
[3] Instruction manual of FT-IR-ATR JASCO Corp. (in Japanese).
[4] A. Ishitani, K. Shoda, H. Ishida, T. Watanabe, K. Yoshida, M. Iwaki, Characterization of oxygen-implanted polyethylene by various analytical techniques, Nucl. Instr. Meth. Phys. Sec. B 39 (1–4) (1989) 783–786.
[5] D.C.L. Vasconcelos, J.A.N. Carvalho, M. Mantel, W.L. Vasconcelos, Corrosion resistance of stainless steel coated with sol–gel silica, J. Non-Cryst. Solid 273 (1–3) (2000) 135–139.
[6] C.J. Brinker, G.W. Scherer, Sol–Gel Science, Academic Press, San Diego, 1990 (Chapter 13).
[7] C.J. Brinker, G.W. Scherer, Sol–Gel Science, Academic Press, San Diego, 1990 (Chapter 9).
[8] T. Sameshima, K. Sakamoto, Y. Tsunoda, T. Saitoh, Improvement of SiO_2 properties and silicon surface passivation by heat treatment with high-pressure H_2O vapor, Jpn. J. Appl. Phys. 37 (1998) L1452–L1454.
[9] P. Innocenzi, Infrared spectroscopy of sol–gel derived silica-based films: a spectra-microstructure overview, J. Non-Cryst. Solid 316 (2–3) (2003) 309–319.
[10] G. Lucovsky, M.J. Manitini, J.K. Srivastava, E.A. Irene, Low-temperature growth of silicon dioxide films: a study of chemical bonding by ellipsometry and infrared spectroscopy, J. Vac. Sci. Technol. B 5 (2) (1987) 530–537.
[11] U. Bräutigam, H. Bürger, W. Vogel, Some aspects of property tailoring of sol–gel derived thin SiO_2 films, J. Non-Cryst. Solid 110 (2–3) (1989) 163–169.
[12] A. Agarwal, M. Tomozawa, W.A. Lanford, Effect of stress on water diffusion in silica glass at various temperatures, J. Non-Cryst. Solid 167 (1–2) (1994) 139–148.
[13] S.P. Mukherjee, D. Suryanarayana, D.H. Strope, Sol–gel processing in electronic packaging materials, J. Non-Cryst. Solid 147 (148) (1992) 783–791.
[14] V.A.C. Haanappel, J.B. Rem, H.D. van Corbach, T. Fransen, P.J. Gellings, Properties of alumina films prepared by metal–organic chemical vapour deposition at atmospheric pressure in the presence of small amounts of water, Surf. Coat. Technol. 72 (1–2) (1995) 1–12.
[15] S. Ghemid, A. Monteil, D. Guichaoua, Orientation of silica rings under uniaxial stress in simulated vitreous silica, Comput. Mater. Sci. 39 (3) (2007) 552–556.
[16] C. Henrist, A. Rulmont, R. Cloots, Synthesis and characterization of inorganic, lamellar nanofillers with high aspect ratio, J. Eur. Ceram. Soc. 27 (2–3) (2007) 1023–1027.
[17] T. Ebina, Nendo wo shuseibun to suru tainetsusei gasubariamaku no kaihatsu, Sansouken TODAY 7 (10) (2007) 18. (in Japanese).
[18] Y.-S. Chou, J.W. Stevenson, P. Singh, Thermal cycle stability of a novel glass-mica composite seal for solid oxide fuel cells: effect of glass volume fraction and stresses, J. Power Sources 152 (2005) 168–174.
[19] G. Majkic, A.J. Jacobson, K. Salama, Stress-induced diffusion and defect chemistry of $La_{0.2}Sr_{0.8}Fe_{0.8}Cr_{0.2}O_{3-\delta}$ Part 3. Defect-chemistry-based modeling, Solid State Ionics 167 (3–4) (2004) 255–262.
[20] D.-H. Yeon, P.-R. Cha, M. Grant, Phase field model of stress-induced surface instabilities: surface diffusion, Acta Mater. 54 (6) (2006) 1623–1630.
[21] D.R. Tallant, T.A. Michalske, W.L. Smith, The effects of tensile stress on the Raman spectrum of silica glass, J. Non-Cryst. Solid 106 (1–3) (1988) 380–383.
[22] O. de Sanctis, L. Gómez, N. Pellegri, C. Parodi, A. Marajofsky, A. Durán, Protective glass coatings on metallic substrates, J. Non-Cryst. Solid 121 (1–3) (1990) 338–343.
[23] S. Iwamori, Y. Gotoh, K. Moorthi, Silicon oxide gas barrier films deposited by reactive sputtering, Surf. Coat. Technol. 166 (1) (2003) 24–30.
[24] T.J. Sarapatka, XPS and XAES study of interaction between Ni and Si(1 1 1), SiO_x/Si(1 1 1) supports, J. Electron Spectr. Rel. Phenom. 62 (4) (1993) 335–349.
[25] H.C. Swart, G.L.P. Berning, The effect of oxygen on the formation of iron silicide, Appl. Surf. Sci. 78 (1) (1994) 77–82.
[26] R.W. Hoffman Jr., T.E. Mitchell, R.W. Hoffman, The structure-mechanical property relationship of amorphous silicon monoxide thin films, Thin Solid Films 154 (1–2) (1987) 149–157.

[27] P. Hones, M. Diserens, F. Lévy, Characterization of sputter-deposited chromium oxide thin films, Surf. Coat. Technol. 120 (121) (1999) 277–283.

[28] S. Matsuno, Effect of Cr content on high temperature corrosion resistance of Fe–Cr alloy, Kurimoto Gihou 47 (2002) 8–11 (in Japanese).

[29] K. Kajihara, T. Miura, H. Kamioka, A. Aiba, M. Uramoto, Y. Morimoto, M. Hirano, L. Skuji, H. Hosono, Diffusion and reactions of interstitial oxygen species in amorphous SiO_2: a review, J. Non-Cryst. Solid 354 (2–9) (2008) 224–232.

[30] W.M. Aylward, P.G. Pickup, Ion-exchange and ion-transport in silica and sulphonated-silica (ormosil) hydrogels, Electrochim. Acta 53 (11) (2008) 3897–3902.

[31] K. Herz, F. Kessler, R. Wächter, M. Powalla, J. Schneider, A. Schulz, U. Schumacher, Dielectric barriers for flexible CIGS solar modules, Thin Solid Films 403 (404) (2002) 384–389.

[32] L. Narváez, O. Dominguéz, J.R. Martínez, F. Ruiz, Preparation of (Ni–B)/SiO_2, Ni/SiO_2 and NiO/SiO_2 nanocomposites, J. Non-Cryst. Solid 318 (1–2) (2003) 37–42.

[33] A.Z. Uedono, Q. Chen, R. Suzuki, T. Ohdaira, T. Mikado, S. Fukui, A. Shiota, S. Kimura, Nanoporous structure of methyl-silsesquioxane films using monoenergetic positron beams, J. Appl. Phys. 90 (5) (2001) 2498–2503.

[34] A. Yae Kina, V.M. Souza, S.S.M. Tavares, J.M. Pardal, J.A. Souza, Microstructure and intergranular corrosion resistance evaluation of AISI 304 steel for high temperature service, Mater. Char. 59 (5) (2008) 651–655.

[35] S.R. Ortner, A stem study of the effect of precipitation on grain boundary chemistry in AISI 304 steel, Acta Metall. Mater. 39 (3) (1991) 341–350.

[36] Y.C. Wu, Y.C. Jean, Hydrogen damage in AISI 304 stainless steel studied by Doppler broadening, Appl. Surf. Sci. 252 (9) (2006) 3278–3284.

[37] H. Rinnert, M. Vergnat, G. Marchal, A. Burneau, Strong visible photoluminescence in amorphous SiO_x and SiO_x: H thin films prepared by thermal evaporation of SiO powder, J. Luminescence 80 (1–4) (1998) 445–448.

[38] W. Hänni, H.E. Hintermann, D. Morel, A. Simmen, Silica coatings on strongly passivated substrates, Surf. Coat. Technol. 36 (1–3) (1988) 463–470.

[39] M. Anas, C. Bellouard, L. Moreau, M. Vergnat, Magnetic and transport properties of annealed Fe(SiO) alloys, J. Magn. Magn. Mater. 284 (2004) 165–171.

[40] F.J. Pérez, E. Otero, M.P. Hierro, C. Gómez, F. Pedraza, J.L. de Segovia, E. Román, High temperature corrosion protection of austenitic AISI 304 stainless steel by Si, Mo and Ce ion implantation, Surf. Coat. Tehnol. 108–109 (1–3) (1998) 127–131.

[41] S. Ono, Y. Nishi, Chromium-free corrosion resistance of metals by ceramic coating, J. Am. Ceram. Soc. 84 (12) (2001) 3054–3056.

[42] A. Pepe, P. Galliano, S. Ceré, M. Aparicio, A. Durán, Hybrid silica sol–gel coatings on Austempered Ductile Iron (ADI), Mater. Lett. 59 (17) (2005) 2219–2222.

[43] F. Bauer, U. Decker, A. Dierdorf, H. Ernst, R. Heller, H. Liebe, R. Mehnert, Preparation of moisture curable polysilazane coatings Part I. Elucidation of low temperature curing kinetics by FT-IR spectroscopy, Prog. Org. Coat. 53 (3) (2005) 183–190.

[44] F. Riffard, H. Buscail, E. Caudron, R. Cueff, C. Issartel, S. Perrier, In-situ characterization of the oxide scale formed on yttrium-coated 304 stainless steel at 1000 °C, Mater. Char. 49 (1) (2002) 55–65.

[45] J.H. Lee, D.S. Kim, Y.H. Lee, B. Farouk, Mechanical properties of a-C:H and a-C:H/SiO_x nanocomposite thin films prepared by ion-assisted plasma-enhanced chemical vapor deposition, Thin Solid Films 280 (1–2) (1996) 204–210.

[46] H. Miyata, T. Noma, M. Watanabe, K. Kuroda, Preparation of mesoporous silica films with fully aligned large mesochannels using nonionic surfactants, Chem. Mater. 14 (2002) 766–772.

[47] J.V. Littlejohns, A.J. Daugulis, Oxygen transfer in a gas–liquid system containing solids of varying oxygen affinity, Chem. Eng. J. 129 (1–3) (2007) 67–74.

[48] K. Izumi, H. Tanaka, Y. Uchida, N. Tohge, T. Minami, Influence of firing conditions on adhesion of methyltrialkoxysilane-derived coatings on steel sheets, J. Non-Cryst. Solid 147 (148) (1992) 483–487.

[49] Japan Patent L2003009732.

[50] A. Pêcheur, J.L. Autran, J.P. Lazarri, P. Pinard, Properties of SiO_2 films deposited on silicon at low temperatures by plasma enhanced decomposition of hexamethyldisilazane, J. Non-Cryst. Solid 245 (1–3) (1999) 20–26.

[51] Website: http://www.infocean.net/qgc/tokusei2.html (accessed Nov. 2007, in Japanese).

[52] S. Okuzaki, K. Okude, T. Ohishi, Photoluminescence behavior of SiO_2 prepared by sol–gel processing, J. Non-Cryst. Solid 265 (1–2) (2000) 61–67.

[53] M. Langlet, D. Walz, P. Marage, J.C. Joubert, SiO_2 thin films deposited by a new sol–gel technique, J. Non-Cryst. Solid 147 (148) (1992) 488–492.

[54] F. Carn, A. Colin, V. Schmitt, F.L. Calderon, R. Backov, Soft matter, sol–gel process and external magnetic field to design macrocellular silica scaffolds, Colloid Surf. A 263 (1–3) (2005) 341–346.

[55] T. Maeseto, T. Kitaoka, S. Toriu, S. Fujii, M. Kobune, Cause of exfoliation of glass lining layer on stainless steel, Kagaku kogaku ronbunshu (in Japanese) 27 (6) (2001) 761–764.

[56] Website: http://www.jst.go.jp/project/concept/report066/report066.html (accessed Feb. 2007, in Japanese).

[57] Website: http://www.jst.go.jp/tt/dokusou/pdf/res_pdf/res_10_2/res_10_2066.pdf (accessed Feb. 2007, in Japanese).

[58] M. Guglielmi, D. Festa, P.C. Innocenzi, P. Colombo, M. Gobbin, Borosilicate coatings on mild steel, J. Non-Cryst. Solid 147 (148) (1992) 474–477.

[59] A.R. Di Giampaolo Conde, M. Puerta, H. Ruiz, J. Lira Olivares, Thick aluminosilicate coatings on carbon steel via sol–gel, J. Non-Cryst. Solid 147 (148) (1992) 467–473.

Makoto Takemori graduated (PhD) in March 1984 from Institute of Industrial Science, the University of Tokyo. From April 1984–March 1985, he was a special research student at the Japan Atomic Energy Research Institute and in April 1985 he was a researcher at AIST.